LASER COOLING OF ATOMS

PACS numbers: 37.10.De; 42.62.Fi
DOI: 10.1070/QE2008v038n10ABEH013794

Study of transitions in thulium atoms in the 410–420-nm range for laser cooling

A.V. Akimov, K.Yu. Chebakov, I.Yu. Tolstikhina, A.V. Sokolov, P.B. Rodionov, S.I. Kanorsky, V.N. Sorokin, N.N. Kolachevsky

Abstract*. The possibility of laser cooling of thulium atoms is considered. The hyperfine structure of almost cyclic $4f^{13}6s^2(J_g = 7/2) \leftrightarrow 4f^{12}5d_{3/2}6s^2(J_e = 9/2)$ and $4f^{13}6s^2(J_g = 7/2) \leftrightarrow 4f^{12}5d_{5/2}6s^2(J_e = 9/2)$ transitions at 410.6 and 420.4 nm, respectively, is studied by the method of sub-Doppler saturation spectroscopy in counterpropagating laser beams. The hyperfine splitting of excited levels involved in these transitions is measured and the natural linewidths of these transitions are determined. The structure of the neighbouring $4f^{13}6s6p(J_e = 5/2)$ and $4f^{12}5d_{5/2}6s^2(J_e = 7/2)$ levels is studied for the first time by this method. The decay probabilities of the $J_e = 9/2$ levels via channels removing atoms from the cooling cycle are calculated. It is found that the branching ratio for the strong transition at 410.6 nm ($A = 6 \times 10^7$ s^{-1}) is smaller than 2×10^{-5}, which makes this transition most promising for laser cooling. The laser cooling of atoms in a Zeeman cooler at this transition is simulated. The possibility of using a laser-cooled cloud of thulium atoms to study the metrological transition at 1.14 μm is discussed.

Keywords: *laser cooling of atoms, saturated absorption spectroscopy, metrological transition, lanthanides.*

1. Introduction

In recent years interest in studies of atoms of the lanthanide group cooled down to low temperatures by laser methods has increased considerably. Cold rare-earth ions can be used both for fundamental investigations, for example, for studying collisions at ultralow temperatures [1] and in applied fields for the development and analysis of nanostructures [2]. Unlike atoms cooled by the buffer gas method demonstrated recently [3], laser-cooled atoms can be easily manipulated with the help of optical fields. Note that not only individual atoms can be manipulated but also one-, two-, and three-dimensional periodically arranged ensembles, for example, by using optical gratings [4]. One of the applications of a source of single atoms is the implantation of atoms into nanostructures, which opens up the possibility for the development of single-photon sources or tensile nanosensors. The use of rare-earth atoms is promising for such studies because the spectral lines of rare-earth ions remain narrow even when they are doped into crystal lattices.

Unlike alkali and alkaline-earth atoms, which are more often used in laser cooling experiments, the spectrum of lanthanides exhibits much more transitions due to the presence of 4f shells, which complicates the study of the evolution of level populations upon laser excitation. Despite this problem, a number of successful experiments on laser cooling of erbium [5] and ytterbium [6–9] atoms have been performed in the USA and Japan. Both these atoms have intense transitions in the 400-nm region, which makes it possible to capture up to 10^6 atoms in a magnetooptical trap (MOT). Note that transitions used for cooling are not closed, i.e. there exists a low probability of decaying the upper excited level into other levels which are not involved to the laser cooling cycle. Such undesirable transitions can considerably affect the possibility of laser cooling of atoms. An ytterbium atom has the closed 4f shell and, therefore, its energy level diagram is simplest. The parasitic decay of the upper $6s6p(^1P_1)$ laser level can occur only to two neighbouring levels whose energies differ by less than 500 cm^{-1}, which suggests [7] that branching will not prevent laser cooling. On the other hand, the energy level diagram of erbium atoms is so complicated that the probability of such undesirable transitions cannot be reliably estimated [5]. However, the efficient laser cooling observed in experiments even in the absence of additional lasers performing the transfer of population from 'dark' sublevels suggests that the above-mentioned parasitic processes do not affect noticeably laser cooling.

In this paper, we consider the possibility of laser cooing of atomic thulium, which is located between erbium and ytterbium in the periodic table. Interest in thulium is caused by a number of reasons. First, to fill completely the 4f shell of a thulium atom (the $4f^{13}6s^2$ ground state), only one electron is required, which makes the energy level diagram of this atom one of the simplest among other lanthanides. Second, the only stable isotope ^{169}Tm has the nuclear spin $I = 1/2$, which leads to the splitting of each electronic level into only two hyperfine levels. The monoisotopic composition of natural thulium suggests that the MOT loading rate can be increased, while the presence of the Zeeman structure of the ground state gives promise that cooling below the Doppler limit can be achieved. Third, it is known that the hyperfine levels of the ground state of rare-earth atoms are screened by the closed $6s^2$ electronic shell, which reduces by

A.V. Akimov, K.Yu. Chebakov, I.Yu. Tolstikhina, A.V. Sokolov, P.B. Rodionov, S.I. Kanorsky, V.N. Sorokin, N.N. Kolachevsky
P.N. Lebedev Physics Institute, Russian Academy of Sciences, Leninsky prosp. 53, 119991 Moscow, Russia; e-mail: alakimov@lebedev.ru

Received 15 January 2007; revision received 12 May 2008
Kvantovaya Elektronika **38** (10) 961–968 (2008)
Translated by M.N. Sapozhnikov

more than four orders of magnitude the collision frequency shifts of transitions between these levels [3, 10]. Thulium has two hyperfine levels in the ground state with total electron moments $J_g = 7/2$ and $J'_g = 5/2$ separated by the frequency interval 2.6×10^{14} Hz corresponding to the wavelength 1.14 μm. Because these levels have the same parity, the electric dipole transition between them is forbidden and the $J'_g = 5/2$ level is metastable, with the lifetime of a few fractions of a second. Such an energy level diagram makes the thulium atom an attractive object for metrological studies and the development of new optical frequency standards because it provides the increase in the signal-to-noise ratio by detecting narrow unperturbed lines in a sufficiently dense atomic ensemble such as a cloud of laser-cooled atoms.

In this paper, we studied experimentally and theoretically transitions in atomic thulium in the spectral range from 410 to 420 nm, which are promising for using in laser cooling schemes.

2. Study of the structure of transitions in thulium atoms in the range from 410 to 420 nm

To provide the efficient laser cooling of atoms, a cyclic transition with the large oscillator strength is required in the spectral region which can be studied with the help of high-power lasers. In the case of thulium atoms, cyclic dipole transitions can occur only from a hyperfine level of the $4f^{13}6s^2$ ground state with $J_g = 7/2$ and the total angular momentum $F = 4$ to the hyperfine levels of excited states with $J_e = 9/2$ and $F = 5$. In this case, electric dipole transitions to other fine and hyperfine levels in the ground state will be forbidden by selection rules.

By analysing possible transitions to the excited even levels [11], we can distinguish three most promising transitions (Table 1): $4f^{12}(^3H_6)5d_{5/2}6s^2$ (18837 cm^{-1}), $4f^{12}(^3F_4)5d_{5/2}6s^2$ (23782 cm^{-1}), and $4f^{12}(^3H_5)5d_{3/2}6s^2$ (24349 cm^{-1}). The longest-wavelength transition at 530.7 nm can be excited by the second harmonic of a Nd : GSGG (gadolinium – scandium – gallium garnet) laser. These lasers are compact, reliable, and do not require expensive pump lasers. In addition, neglecting nonresonance perturbations and unlikely collision processes resulting in the spin flip this transition is completely cyclic. However, the relatively low probability of this transition (2.3×10^6 s^{-1}) complicates its use for the efficient loading of a MOT. The other two transitions lie in the blue spectral region and can be excited by the second harmonic of a Ti : sapphire laser, the second harmonic of high-power semiconductor lasers or by radiation from blue semiconductor lasers. The probabilities of these transitions at 420.4 an 410.6 nm are 2.5×10^7 and 6×10^7 s^{-1}, respectively, which is sufficient for the efficient cooling of atoms from a thermal beam at distances less than 0.5 m. However, these transitions are not completely cyclic and the upper levels can decay to neighbouring odd levels (Table 1).

We investigated the hyperfine structure of transitions at 420.4 and 410.6 nm by the method of saturated absorption spectroscopy in counterpropagating beams. The hyperfine structure of the excited levels in thulium is presented in [12 – 15]. We developed a laser cooling scheme and obtained the reliable experimental estimate of the probability of these transitions, which is important for analysis of laser cooling processes [16].

Figure 1 presents the scheme of experiments. Excitation was performed by a laser system consisting of a Coherent MBR-110 Ti : sapphire laser pumped by the second harmonic of a Coherent Verdi-10 Nd : YVO_3 laser, whose frequency was doubled in a lithium triobate crystal (LBO) placed into an external Coherent MBD-200 resonator. The system generated ~ 100 mW of cw radiation in the range from 400 to 425 nm without the replacement of optical elements. The system was preliminarily tuned to the transition under study with the help of a wavelength meter based on a Michelson interferometer which was manufactured in our laboratory and provided the wavelength

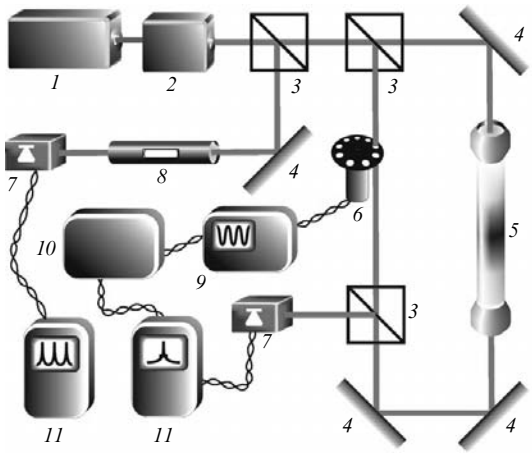

Figure 1. Scheme of the experimental setup for studying the hyperfine structure of thulium: (*1*) laser system; (*2*) frequency doubler; (*3*) beamsplitter cube; (*4*) mirror; (*5*) cell (to which a longitudinal magnetic field can be applied); (*6*) chopper; (*7*) photodiode; (*8*) interferometer providing a distance of 75 MHz between frequency marks; (*9*) master oscillator; (*10*) lock-in detector; (*11*) digital oscilloscope.

Table 1. Some energy levels of thulium (without the hyperfine structure).

Odd levels	J	Energy/cm^{-1}	Even levels	J	Energy/cm^{-1}
$4f^{13}(^2F^o)6s^2$	7/2	0	$4f^{12}(^3H_6)5d_{5/2}6s^2(6,5/2)$	9/2	18837
$4f^{13}(^2F^o)6s^2$	5/2	8771	$4f^{12}(^3F_4)5d_{5/2}6s^2(4,5/2)$	7/2	23782
$4f^{13}(^2F^o_{7/2})5d6s(^3D)^3[11/2]^o$	9/2	22420	$4f^{12}(^3F_4)5d_{5/2}6s^2$	7/2	23873
$4f^{12}(^3H_6)6s^26p_{1/2}(6,1/2)^o$	11/2	22468	$4f^{12}(^3H_5)5d_{3/2}6s^2(5,3/2)$	9/2	24349
$4f^{13}(^2F^o_{7/2})5d6s(^3D)^3[11/2]^o$	11/2	22560	$4f^{13}(^2F^o_{7/2})6s6p(^1P^o_1)(7/2,1)$	5/2	24418
$4f^{13}(^2F^o_{7/2})5d6s(^3D)^3[5/2]^o$	7/2	23335			
$4f^{13}(^2F^o_{7/2})5d6s(^3D)^3[7/2]^o$	9/2	23941			

Note: J is the total electron moment.

measurement error $\Delta\lambda/\lambda = 10^{-6}$. This allowed us to find easily a Doppler line by observing visually a luminescence signal. The laser system has a broad continuous tuning range (up to 40 GHz) and emits the line of width ~ 200 kHz (according to specification), which is achieved by stabilising the laser frequency with respect to a built-in Fabry–Perot resonator.

The radiation beam from the Ti:sapphire laser is attenuated and is split into a saturating and probe beams, which are coupled into a cell strictly toward each other. The possible nonparallel propagation of the beams and their divergence do not exceed 5×10^{-4} rad. The saturating beam is modulated with a chopper, and the probe beam is detected with a lock-in detector at the modulation frequency. The frequency detuning of the laser radiation is controlled with a confocal Fabry–Perot interferometer. The interferometer was calibrated by the known splitting frequency of the $4f^{13}6s^2(J_g = 7/2)$ ground state of thulium equal to 1496.550(1) MHz [12]. The synchronous recording of saturated absorption spectra and the transmission signal of the interferometer provides stable frequency marks in spectra.

A thulium cell is made of a stainless steel tube of diameter 20 m and length 0.6 m with tilted fused silica windows at the ends, which contains several metal thulium grains (a few hundred milligrams) placed at the centre. The cell is continuously evacuated by a turbomolecular pump of capability 30 L s^{-1} down to a pressure of $\sim 10^{-5}$ mbar, which is measured with an Ionivac ITR90 pressure gauge. On the central part of the tube about 20 coils of a coaxial thermoelectric cable are wound, which are electrically isolated from the tube by mica plates. The cable is fed by a direct current, magnetic fields being minimised by passing the current sequentially through the cladding and central core of the cable. Around the heater a few layers of heat-insulating material are coiled, which alternate with nickel foil layers. Temperature is controlled within $\sim 1\,^{\circ}$C with the help of a feedback loop by a signal from a thermocouple. To avoid the heating of the entire tube, several copper tube coils, through which water circulates continuously, are soldered on both ends of the heater.

Thulium, as other rare-earth elements, has the high melting temperature (1818 K); however, a high enough thulium vapour pressure is achieved at lower temperatures. Thus, the luminescence of thulium vapour in our cell was observed already at a temperature of ~ 1000 K, and absorption at the maximum of the 410.6-nm line for one beam at 1100 K achieved 30 %. In this regime, the thulium cell provided stable absorption during 5–6 hours of continuous operation. The setup can also provide the application of a longitudinal magnetic field on the vapour region with the help of Helmholtz coils.

Figure 2 presents the saturated absorption spectra of thulium vapour for four transitions at 409.4, 410.6, 418.9, and 420.4 nm. The shape of the spectrum weakly depends

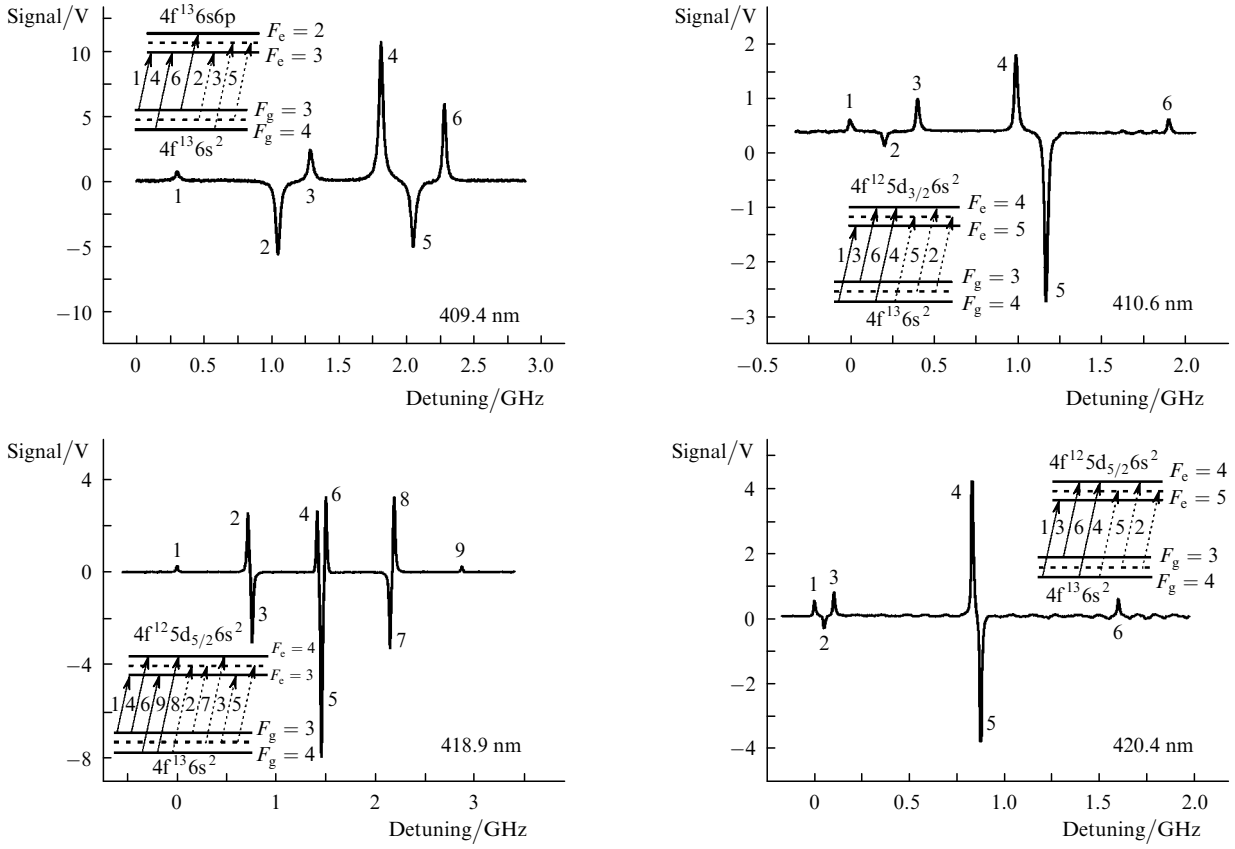

Figure 2. Saturated absorption spectra of thulium vapour recorded in counterpropagating beams of the same frequency with linear orthogonal (409.4 nm) and parallel (410.6, 418.9, and 420.4 nm) polarisations. Each spectrum has its own frequency scale origin. The solid straight lines in insets indicate energy levels; the solid arrows show transitions between them; the dashed straight lines show effective levels with energies equal to half-sums of the energies of the corresponding real levels; the dotted arrows show transitions corresponding to cross resonances. The figures at the arrows and curves are the numbers of transitions and resonances. The saturated absorption resonances correspond to the positive signal, while optical pumping resonances correspond to the negative signal ($F_{g,e}$ are the total angular momenta of the ground and excited states).

on the choice of parallel or orthogonal linear polarisations of the saturating and probe beams. The spectra of lines at 410.6, 418.9, and 420.4 nm are recorded for linear perpendicular polarisations of the saturating and probe beams, and at 409.4 nm – for parallel polarisations. The residual magnetic field in the cell was fractions of gauss. The cross section of astigmatic Gaussian beams at the cell centre at the $1/e^2$ level was 3×6 mm and their power was varied from 10 μW to several milliwatts.

Except saturated absorption resonances formed by atoms with the zero velocity projection on the cell axis, the spectrum also exhibited cross resonances [17] at the frequency equal to the half-sum of frequencies of the corresponding saturated absorption resonances. The sign of cross resonances depends on the mechanism of population transfer between sublevels.

The origin of signs of resonances can be conveniently explained by the example of the 409.4-nm line. When the frequencies of light fields are equal to the half-sum of the frequencies of transitions 1 and 4 (Fig. 2), there exists a group of atoms with such velocities that the high-power wave interacts with transition 1 and the probe wave interacts with transition 4. The high-power laser radiation transfers the population from the $F_g = 4$ sublevel of the ground state to the $F_g = 3$ sublevel during optical pumping. In this case, the absorption of the weak wave at transition 4 increases. At the same frequency, there exists a group of atoms with such velocities that the high-power wave interacts with transition 4 and the probe wave interacts with transition 1. It is obvious that absorption for this group of atoms also increases. Thus, the sign of cross resonance 2 should be opposite to the sign of saturated absorption resonances. This also concerns the sign of resonance 5 between lines 4 and 6, which appears when the laser is tuned to the frequency difference of the 'middle lines' of the upper and lower levels. Knowing the order and signs of resonances, we can completely interpret the spectrum. The correctness of the assignment of resonances was additionally verified by the Zeeman splitting of resonances in a longitudinal magnetic field with the induction 20 G and also by the relative intensities of transition lines. The assignment of the resonances is presented in insets in Fig. 2.

Transition frequencies were determined by approximating spectra by a Lorentzian with the required number of peaks. The frequency measurement error is a sum of the statistical error (~ 0.5 MHz) and systematic error (~ 0.5 MHz) related mainly to the asymmetry of transmission peaks of the confocal interferometer. The systematic error was estimated by analysing the positions of cross resonances. Note that the systematic error is independent of the hyperfine splitting value. Hyperfine splittings of four excited levels of a thulium atom obtained from the spectra are presented in Table 2. Three hyperfine splittings are measured for the first time, while the hyperfine splitting obtained for the 410.6-nm line is consistent with previous measurements and refine them.

It is interesting that the hyperfine splitting for both candidates for laser cooling (transitions at 410.6 and 420.4 nm) is almost the same, the splitting of upper levels being somewhat larger. Because the laser cooling of atoms should occur at the cyclic $F_g = 4 \rightarrow F_e = 5$ transition with a small red frequency detuning, the cooling radiation should also weakly interact with the $F_g = 3 \rightarrow F_e = 4$ transition, by fulfilling the functions of population transfer radiation, which is necessary for cooling alkali atoms (for example, Rb and Cs). Indeed, the population transfer to the $F_g = 3$ 'dark' sublevel of the ground state occurs mainly due to nonresonance excitation of the $F_g = 4_e = 4$ transition. The probability of such a process is determined by the ratio of the laser linewidth to the splitting of the upper sublevels with $F_e = 4$ and 5. The probability of the 'reverse' process of optical pumping with the $F_g = 3$ sublevel to the $F_g = 4$ sublevel of the ground state is determined by the probability of nonresonance absorption from the $F_g = 3$ level to the $F_e = 4$ level, i.e. by the splitting of lower sublevels. Due to the specific structure of levels of the thulium atom, the 'reverse' process proves to be more probable. This effect was demonstrated by the authors of paper [5], which have managed to capture up to 10^6 erbium atoms in a trap without using a laser for population transfer.

An important parameter determining the cooling efficiency and the minimal achievable temperature of atoms is the decay probability of the upper level of the cooling transition. This parameter in our experiments can be determined from the resonance width corresponding to the zero radiation power (Fig. 3). The line full width at half-maximum γ was determined by approximating the line profiles by Lorentzians.

The dependence of the linewidth γ on the exciting radiation intensity I for cyclic $F_g = 4 \rightarrow F_e = 5$ transitions, which can be approximately described by a two-level model in the case of a weak saturating beam [17–19], has the form

$$\gamma(I) = \frac{1}{2}\,\gamma_0\left[1 + \left(1 + \frac{I}{I_{\mathrm{sat}}}\right)^{1/2}\right], \qquad (1)$$

where γ_0 is the natural linewidth; $I_{\mathrm{sat}} = 2\pi hc\gamma_0/(3\lambda^3)$ is the saturation intensity; h is Planck's constant; and c is the speed of light.

The approximation of data presented in Fig. 3 by expression (1) gives $\gamma_0^{\mathrm{exp}}(410.6\ \mathrm{nm}) = 10.5 \pm 2$ MHz and $\gamma_0^{\mathrm{exp}}(420.4\ \mathrm{nm}) = 3.8 \pm 1$ MHz for the $F_g = 4 \leftrightarrow F_e = 5$ transitions. Due to a large uncertainty of the exciting radiation intensity and its inhomogeneous distribution in

Table 2. Hyperfine splitting of the ground and four excited even levels of a thulium atom.

Energy/cm^{-1}	Wavelength/nm	Excited level	J_e	Splitting/MHz	References
0	–	$4f^{13}6s^2(^2F^o)$	7/2	-1496.550 ± 0.001	[12]
23781	420.4	$4f^{12}(^3F_4)5d_{5/2}6s^2$	9/2	-1586.6 ± 0.8	This paper
23873	418.9	$4f^{12}(^3F_4)5d_{5/2}6s^2$	7/2	$+1411.0 \pm 0.7$	This paper
24348	410.6	$4f^{12}(^3H_5)5d_{3/2}6s^2$	9/2	-1856.5 ± 2.5 -1857.5 ± 0.8	[16] This paper
24418	409.4	$4f^{13}(^2F^o_{7/2})6s6p(^1P^o_1)$	5/2	-1969.4 ± 1.3	This paper

Note: the splitting sign corresponds to the Fermi energy sign and is positive when energy increases with increasing the total angular momentum F.

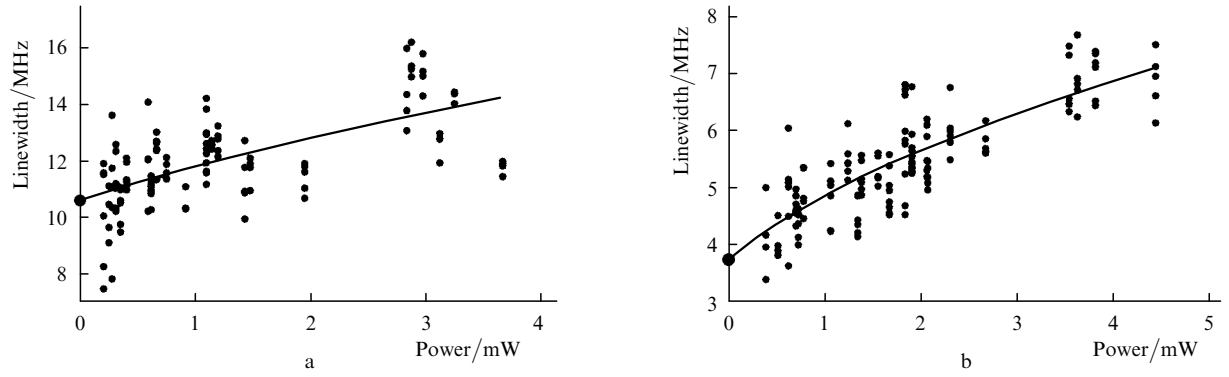

Figure 3. Dependences of the line FWHM γ on the radiation power for transitions at 410.6 nm (a) and 420.4 nm (b). Solid curves are the approximation of data by theoretical dependence (1).

the laser beam, we used I_{sat} as a fitting parameter along with γ_0.

Table 3 presents the decay probabilities of transitions from the upper levels of thulium atoms at 410.6 and 420.4 nm, obtained by using the procedure described above. The probabilities were calculated taking into account systematic broadenings of the spectral lines. The main systematic contribution is the laser linewidth equal to 0.2 ± 0.2 MHz according to the manufacturer specification (assuming that the main noise source is the acoustic noise with a long correlation time, we doubled the linewidth of the Ti : sapphire laser [20]). The time-of-flight broadening also introduces a noticeable contribution (0.1 ± 0.1 MHz). A comparable broadening is produced by the residual constant magnetic field in the cell. Because of the almost identical g-factors of the upper and lower levels, the splitting for π-components is virtually absent. For σ-components, the splitting (in megahertz) is $\Delta\nu = 1.5B$, where B is the magnetic field induction (in gauss). For $B = 1$ G, this splitting is small compared to the linewidth and leads to its inhomogeneous broadening described by the expression $(\gamma_0^2 + \Delta\nu^2)^{1/2}$, which corresponds to 0.1 ± 0.2 MHz. The geometrical broadening appearing due to the possible presence of an angle between laser beams does not exceed 10 ± 10 kHz. The collision shift is also negligibly small (50 ± 50 kHz). Taking into account all these contributions, we obtain finally $\gamma_0^{exp}(410.6\text{ nm}) = 10.0 \pm 0.4$ MHz and $\gamma_0^{exp}(420.4\text{ nm}) = 3.3 \pm 0.4$ MHz.

3. Analysis of the possibility of cooling thulium atoms

We estimated the branching ratio for the decay of the upper levels of transitions at 410.6 and 420.4 nm by using the COWAN program [21] for calculating the energy levels of many-electron neutral atoms and determining the probability of corresponding electric dipole transitions. It was taken into account that electronic configurations of the thulium atom are not pure. Calculations were performed (Table 3) for all allowed electric dipole transitions from two excited even levels (24 349 and 23 782 cm^{-1}) to lower odd levels (see Table 1) and can be used only for approximate estimates because the thulium atom is an extremely intricate quantum-mechanical system. Note that the possibility of cooling erbium [5] and ytterbium [7] atoms was estimated without estimating the branching ratio.

Table 3 shows that the COWAN program provides adequate calculations of the energy levels and gives the plausible estimate of the probability of known transitions. The probability of the transition at 410.6 nm exceeds its

Table 3. Probabilities of electric dipole transitions in a thulium atom from the $4f^{12}(^3H_5)5d_{3/2}6s^2$ ($E_e^{NIST} = 24349$ cm^{-1}) and $4f^{12}(^3F_4)5d_{5/2}6s^2$ ($E_e^{NIST} = 23782$ cm^{-1}) levels to different odd levels.

$E_g^{COWAN}/10^3$ cm^{-1}	$E_g^{NIST}/10^3$ cm^{-1}	J_g	$E_e^{COWAN}/10^3$ cm^{-1}	$E_e^{NIST}/10^3$ cm^{-1}	J_e	A^{COWAN}/s^{-1}	A^{NIST}/s^{-1}	A/s^{-1}
0	0	7/2	24.341	24.349	9/2	2.13×10^8	$6.38(30) \times 10^7$	$6.3(3) \times 10^7$
22.166	22.420	9/2	24.341	24.349	9/2	4.44×10^2		
22.243	22.468	11/2	24.341	24.349	9/2	1.75×10^2		
22.417	22.560	11/2	24.341	24.349	9/2	1.82×10^2		
22.905	23.335	7/2	24.341	24.349	9/2	1.38×10^2		
23.622	23.941	9/2	24.341	24.349	9/2	1.54×10^1		
23.893	23.873	7/2	24.341	24.349	9/2	2.95×10^0		
0	0	7/2	23.797	23.782	9/2	2.27×10^7	$2.43(12) \times 10^7$	$2.1(3) \times 10^7$
22.166	22.420	9/2	23.797	23.782	9/2	1.88×10^1		
22.243	22.468	11/2	23.797	23.782	9/2	1.81×10^2		
22.417	22.560	11/2	23.797	23.782	9/2	8.64×10^2		
22.905	23.335	7/2	23,797	23.782	9/2	1.13×10^0		

Note: $E_{g,e}^{COWAN}$ and A^{COWAN} are the level energies and corresponding probabilities obtained by using the COWAN program [21]; $E_{g,e}^{NIST}$ and A^{NIST} are experimental values taken from the NIST data base (National Institute of Standards and Technologies, USA) [11]; A are the transition probabilities obtained in this paper.

experimental value approximately by three times, which can be considered as the estimate of the accuracy of this calculation. By summing the probabilities of all undesirable decay channels (all the channels except the decay to the ground state) and normalising them to the total decay probability, we obtain the estimate of branching ratios k:

$$k(410.6\ \text{nm}) = 1^{+1}_{-0.5} \times 10^{-5}, \quad (2)$$

$$k(420.4\ \text{nm}) = 5^{+5}_{-2.5} \times 10^{-5}, \quad (3)$$

where the confidence interval estimates the calculation error. It is also necessary to take into account the fact that not all the atoms decaying to odd levels with energies from 22000 to 24000 cm^{-1} are completely removed from a cooling cycle. A part of these atoms can decay to lower even levels and atoms can return to the ground state with $J_g = 7/2$. According to [5], such cascade decays can be treated as a population 'reservoir' slowly feeding the ground state. The numerical estimate of the probability of such processes is a cumbersome problem, and therefore we will consider estimates (2) and (3) as the upper boundary of the relative probability of population depletion during cooling.

We estimated the probability of the $J_g = 7/2 \rightarrow J'_g = 5/2$ metrological transition at 1.14 μm. The probability of the magnetic dipole transition calculated by using the COWAN program is 5.9 s^{-1}, while the probability of this transition calculated by using the Flexible Atomic Code [22] is 7.7 s^{-1}. According to data from [3], the cross section for inelastic scattering perturbing the population of the fine levels of the ground state is at least four orders of magnitude lower than the elastic scattering cross section for transitions between the s- and p-shells. Therefore, during the natural lifetime only several atoms of the total number of atoms confined in a trap will be lost. The linewidth of the metrological transition is ~ 1 Hz and corresponds to the potential Q factor of 2×10^{14}. Although this value is inferior to the Q factors of some metrological transitions in ions [23], the possibility of detecting a signal from a large atomic ensemble will provide a short accumulation time of the signal [4]. The transition can be excited either by the second harmonic from Tm : YAG or Tm : YLF (2.3 μm) lasers or by radiation from fibre lasers. Note that the methods of narrowing of laser linewidths down to subhertz values became now a standard procedure [24]. The transition can be also used as a reference for a frequency standard based on the coherent population trapping resonance [25]. In this case, the transitions at 418.9 and 409.4 nm studied in our paper can be used.

It follows from Table 3 that the 410.6-nm transition provides the more efficient cooling of atoms than the 420.4-nm transition because its probability is approximately twice that of the latter transition and it has a lower branching ratio [cf. (2) and (3)]. Below, we consider the possibility of slowing down thulium atoms by using resonance radiation at 410.6 nm. As follows from this consideration, the second transition is inconvenient for cooling of atoms.

To perform the efficient loading of a MOT, it is necessary to cool preliminarily a beam, which is achieved by using a Zeeman moderator (see, for example, [26]). The operation of the moderator is based on irradiation of a collimated atomic beam by a counterpropagating resonance circularly polarised laser beam; the frequency shift caused by the Doppler shift varying in time is compensated by the Zeeman shift of the levels (Fig. 4). It is easy to show that to cool preliminarily thulium atoms with the initial velocity of 200 m s^{-1}, it is necessary to scatter ~ 35000 photons. The estimate for the 420.4-nm transition by (3) shows that all the atoms are virtually lost in the preliminary cooling, whereas the expected losses at the 410.6-nm transition do not exceed 35 %.

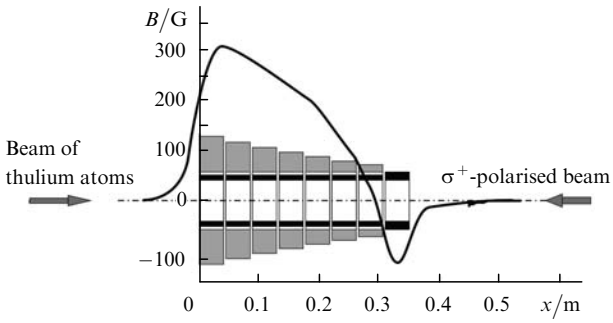

Figure 4. Design of a sectional Zeeman cooler and the profile of a magnetic field produced by the cooler. The internal diameter of the cooler is 2 cm. Currents in coils indicated in black and grey flow in the opposite directions.

We calculated a Zeeman moderator for thulium atoms at the cooling transition at 410.6 nm the σ^+-polarised light [26]. The cooler was calculated by selecting the axially symmetric configuration of coils so that the axial distribution of their magnetic field would best correspond to the theoretical curve providing the slowing down of atoms at the maximal acceleration for the specified radiation intensity close to the saturating intensity.

After the calculation of the field on the axis, we solved numerically the equation of motion for an atom with the initial velocity v_{fin} flying up to the moderator from a source of atoms (furnace). As a result, the final velocity v_{fin} of the atom near the MOT was determined. The length of the sectional cooler used in calculations was ~ 35 cm.

Figure 5 shows how the calculated Zeeman moderator transforms the Maxwell velocity distribution in a collimated atomic beam escaping from a furnace at a temperature of 1100 K. It was assumed that the transition saturation parameter was much greater than unity and the reemission probability was close to $A/2$. One can see that most of the atoms with velocities below a cut-off velocity are transferred to a group of atoms at velocities ~ 40 m s^{-1} in the MOT region. A part of initially slow atoms is reflected backward. A fraction of atoms in a narrow peak is ~ 11 %, which suggests that the efficient loading of the MOT can occur. Because to slow down atoms at the velocity $v_{\text{in}} = 200$ m s^{-1}, it is necessary to scatter $\sim 3.5 \times 10^4$ resonance photons, the radial velocity (~ 2 m s^{-1}) can be neglected compared to the axial velocity at the cooler output.

Taking result (2) into account, we can conclude that during slowing down the fraction of atoms lost due to parasitic decays from upper levels can amount to ~ 35 %. Nevertheless, even for such a conservative estimate, the cooler can provide a flow of a great number of atoms to the MOT (estimated as $10^7 - 10^8$ at $^{s-1}$, the amount of atoms being considerably dependent on the geometry of light fields in the MOT and the collimation of the atomic beam). Our

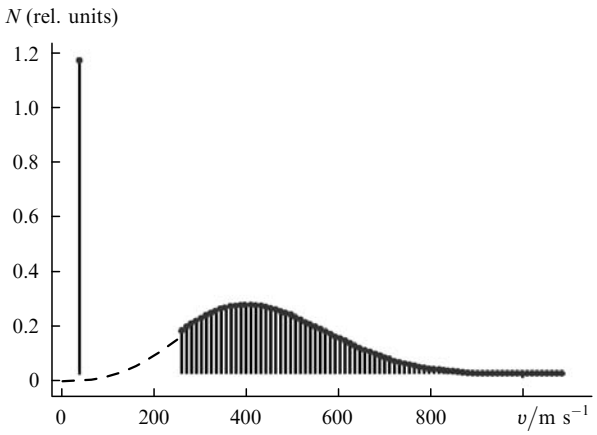

Figure 5. Velocity distributions of atoms at the input (dashed curve) and output (dots) of a cooler. Dots are plotted with a step of 10 m s^{-1}. The peak corresponding to the velocity 39 m s^{-1} contains ~ 11 % of atoms. Beginning from the velocity ~ 250 m s^{-1}, the input and output distributions coincide.

analysis shows that in the case of the 420.4-nm transition, the atoms are almost completely lost due to parasitic decay channels. The total number of atoms that can be captured in the MOT depends on the trap geometry and on losses caused by collisions of these atoms with hot atoms in the beam and background gas atoms.

The temperature that can be achieved in a MOT corresponds to the so-called Doppler limit $T_D = \hbar A/(2k_B)$, where k_B is the Boltzmann constant. Table 4 shows that the velocity corresponding to this temperature for the 410.6-nm transition is too high for measuring the metrological transition of atoms in a ballistic flight. This regime is achieved by switching off the light and magnetic fields in the MOT; however, in the given case, a cloud of atoms will fly apart in the radial direction before their trajectories will be subjected to the gravitational field [27]. To record the narrow metrological transition line, it is desirable to provide the interaction time of atoms with radiation at 1.14 μm equal to 0.1 – 1 s. Because the ground state of thulium has the Zeeman structure, a further cooling can be performed by using, for example, the Sisyphus cooling mechanism in an optical molasses. In this case, temperature can be lowered down to the limiting temperature $T_{rec} = h^2/(2m\lambda^2 k_B)$ (where m is the atom mass) determined by the recoil effect. In addition, another, completely closed and weaker cooling transition at 530.6 nm can be used (as was done in [7]), which considerably reduces the Doppler limit and the average velocity of atoms in the cloud.

Particles at such temperatures can be loaded into an optical grating or captured by optical tweezers usually representing a dipole trap of depth ~ 100 K, which allows the manipulation by thulium atoms.

Table 4. Temperatures corresponding to the Doppler limit of cooling T_D and to the limit determined by the recoil effect T_{rec} for two cooling transitions.

λ/nm	A/s^{-1}	$T_D/\mu K$	υ_D/cm s^{-1}	T_{rec}/nK	υ_{rec}/cm s^{-1}
410.6	6×10^7	230	15	330	0.6
530.7	2.3×10^6	9	3	200	0.4

Note: υ_D and υ_{rec} are the most probable velocities for thermal distributions corresponding to presented temperatures.

4. Conclusions

We have analysed the possibilities of cooling thulium atoms at transitions in the spectral range from 410 to 420 nm. The spectra of four intense transitions have been recorded by the method of saturated absorption in counterpropagating beams. The hyperfine splitting of the excited levels with energies 23782, 23873, and 24418 cm^{-1} has been measured for the first time and the hyperfine splitting of the 24349-cm^{-1} level has been refined. The natural linewidth is measured for the 410.6-nm and 420.4-nm transitions, which can be used as cooling transitions. The results of the measurements are consistent with data presented in [11].

The theoretical analysis of the branching ratios for the decay of the upper levels of cooling transitions has shown that the 410.6-nm transition is most promising for cooling thulium atoms. It is shown that, by using radiation at this wavelength, it is possible to reduce efficiently the velocity of 11 % of thulium atoms in a beam with the initial temperature 110 K down to 40 m s^{-1} with the help of a Zeeman cooler of length 35 cm.

We have proposed the following scheme for cooling and detecting thulium atoms: slowing down in a Zeeman cooler by using resonance radiation at 410.6 nm; the capture of atoms in a MOT; switching off the MOT and additional cooling of atoms in an optical molasses or in the MOT by using laser radiation at 530.7 nm; and recording of the $F_g = 4 \rightarrow F_g = 3$ transition at 1.14 μm.

The Q factor of the magnetic dipole transition at 1.14 μm is 2×10^{14}, which makes it possible to develop a precise optical clock featuring a high short-term stability. In the nearest future our group begins to study the cooling of thulium atoms in a Zeeman cooler and to assemble a MOT. We will also consider the possibility of using the capture of atoms in an optical dipole trap.

Acknowledgements. This work was supported by the Russian Foundation for Basic Research (Grant Nos 05-02-16801 and 07-02-00492), the Foundation for Support of the Russian Science, and the Alexander von Humboldt Foundation.

References

1. Santos L., Shlyapnikov G.V., Zoller P., Lewenstein M. *Phys. Rev. Lett.*, **85**, 1791 (2000).
2. Hill S.B., McClelland J.J. *Appl. Phys. Lett.*, **82**, 3128 (2003).
3. Hancox C.I., Doret S.C., Hummon M.T., Luo L., Doyle J.M. *Nature*, **431**, 281 (2004).
4. Katori Hidetoshi, Takamoto Masao, Pal'chikov V.G., Ovsjannikov V.D. *Phys. Rev. Lett.*, **91**, 173005 (2003).
5. McClelland J.J., Hanssen J.L. *Phys. Rev. Lett.*, **96**, 143005 (2006).
6. Loftus T., Bochinski J.R., Shivitz R., Mossberg T.W. *Phys. Rev. A*, **61**, 051401R (2000).
7. Maruyama R., Wynar R.H., Romalis M.V., Andalkar A., Swallows M.D., Pearson C.E., Fortson E.N. *Phys. Rev. A*, **68**, 011403R (2003).
8. Hoyt C.W., Barber Z.W., Oates C.W., Fortier T.M., Diddams S.A., Hollberg L. *Phys. Rev. Lett.*, **95**, 083003 (2005).
9. Fukuhara Takeshi, Takasu Yosuke, Kumakura Mitsutaka, Takahashi Yoshiro. *Phys. Rev. Lett.*, **98**, 030401 (2007).
10. Aleksandrov E.B., Kotylev V.N., Kulyasov V.N., Vasilevskii K.P. *Opt. Spektrosk.*, **54**, 3 (1983).
11. http://www.physics.nist.gov/PhysRefData/ASD/index.html.
12. Childs W.J., Crosswhite H., Goodman L.S., Pfeufer V. *J. Opt. Soc. Am. B*, **1** (1), 22 (1984).

13. Van Leeuwen K.A.H., Eliel E.R., Hogervorst W. *Phys. Lett. A*, **78**, 54 (1980).
14. Pfeufer V. *Z. Phys. D*, **4**, 351 (1987).
15. Kröger S., Tanriver L., Kronfeldt H.-D., Guthöhrlein G., Behrens H.-O. *Z. Phys. D*, **41**, 181 (1997).
16. McClelland J.J. *Phys. Rev. A*, **73**, 064502 (2006).
17. Letokhov V.S., Chebotaev V.P. *Principles of Nonlinear Laser Spectroscopy* (Heidelberg: Springer-Verlag, 1977; Moscow: Nauka, 1975).
18. Pappas P.G., Burns M.M., Hinshelwood D.D., Fels M.S. *Phys. Rev. A*, **21**, 1955 (1980).
19. Ohshima S.I., Nakadan Y., Koga Y. *IEEE J. Quantum Electron.*, **23**, 473 (1987).
20. Rytov S.M., Kravtsov Yu.A., Tatarski M.I. *Vvedenie v statisticheskuyu radiofiziku* (Introduction to Statistical Radiophysics) (Moscow: Nauka, 1978) Vol. 2.
21. Cowan R.D. *The Theory of Atomic Structure and Spectra* (Berkeley, CA: California University Press, 1981).
22. Gu Ming Feng. *Proc. 14th APS Topical Conf. on Atomic Processes in Plasmas* (Santa Fe, NM: AIP Conf. Proc., 2004) Vol. 730, pp 127 – 136.
23. Riehle F. *Frequency Standards. Basics and Applications* (Weinhein, Germany: Wiley-VCH Verlag GmbH, 2004).
24. Ludlow A.D., Huang X., Notcutt M., Zanon-Willette T., Foreman S.M., Boyd M.M., Blatt S., Ye J. *Opt. Lett.*, **32** (6), 641 (2007).
25. Akimov A.V., Matveev A.N., Sokolov A.V., Tereshenko E.O., Kondratjev D.A., Sorokin V.N., Kanorsky S.I., Kolachevsky N.N. *J. Raman Spectrosc.*, **37** (6), 712 (2006).
26. Barrett T.E., Dapore-Schwartz S.W., Ray M.D., Lafyatis G.P. *Phys. Rev. Lett.*, **67**, 3483 (1991).
27. Morinaga A., Riehle F., Ishikawa J., Helmcke J. *Appl. Phys. B*, **48**, 165 (1989).